

Towards multifunctional heterostructured materials: ZnO nanowires growth on mesoscale periodically patterned Si

Anisha Gokarna^{*,1}, Agnieszka Gwiazda^{***,1}, Hind Kadiri^{***,1,2}, Anna Rumyantseva¹, Komla Nomenyo¹, Roy Aad¹, and Gilles Lerondel^{***,1}

¹ Laboratoire de Nanotechnologie et d'Instrumentation Optique, Institut Charles Delaunay, CNRS UMR 6281, Université de Technologie de Troyes, 12 rue Marie Curie, BP 2060, 10010 Troyes, France

² SILSEF Archamps Technopole, 74160 Archamps, France

Received 16 November 2015, revised 20 April 2016, accepted 22 April 2016

Published online 6 May 2016

Keywords laser interference lithography, zinc oxide, silicon, X-ray diffraction, nanosphere lithography, multifunctional materials

* Corresponding author: e-mail anisha.gokarna@utt.fr,

** e-mail gilles.lerondel@utt.fr

*** Equal contribution from both these co-authors.

We report the growth of ZnO nanowires on mesoscale periodically patterned silicon. The aim of this work is to go towards fabrication of multifunctional heterostructured materials for increasing the specific surface area and light absorption properties. ZnO nanowires (NWs) were grown by chemical bath deposition technique on

patterned silicon. Silicon patterning was conducted by two methods, namely, laser interference lithography and nanosphere lithography. We have studied the structural and optical properties of the ZnO NWs grown on these silicon patterns.

© 2016 WILEY-VCH Verlag GmbH & Co. KGaA, Weinheim

1 Introduction Application-oriented nanomaterial design and fabrication are highly necessary and are turning into a new trend nowadays. ZnO nanostructures, such as nanowire arrays (NWAs), have attracted a great deal of research interest over the past few years due to their unique properties and exciting potential applications in nanogenerators [1], piezotronics [2], UV lasers [3], light emitting diodes [4], solar cells [5], and sensors [6]. Compared to one-dimensional (1D) nanostructures or core-shell nanowire heterostructures, branched heterostructures are very promising candidates for nanodevice building blocks due to the enhanced surface area and improved light absorption [7]. In addition, the smaller size of the NW branches (compared to the larger size of NW backbones) can also result in higher efficiency of carrier separation and collection.

To meet the diverse needs of nanodevice structure and function, each of the applications mentioned before requires a different arrangement, density and morphology of ZnO NWAs. Therefore, the ability to produce large-scale

highly ordered ZnO NWAs with the desired position, diameter, orientation, arrangement, density and morphology is essential for the integration and optimization of related functional nano or micro devices. Various patterning methods such as optical lithography [8], nanosphere lithography (NSL) [9, 10], nanoimprint lithography (NIL) [11, 12], and laser interference lithography (LIL) [13, 14] have been employed to provide templates and bring order to the growth of ZnO NWs, so called patterned growth. Among these methods, NSL and LIL are of special interest as they allow for rather simple large scale fabrication as compared to other lithographic methods. Even NSL can lead to long distance ordering if combined with a pre-patterning [15].

In this present work, ZnO NWs have been obtained on large scale pre-patterned silicon templates. The micro- and mesoscale silicon patterns were fabricated using LIL and NSL techniques (using polystyrene beads) in combination with silicon reactive ion etching. ZnO NWs were grown on the silicon patterns by chemical bath deposition technique. The growth behavior and the structural and optical proper-

ties of these ZnO NWs grown on these patterned substrates have been studied.

2 Experiments

2.1 Structured Si patterns (meso-patterns) using laser interference lithography For the formation of Si patterns, we used LIL technique. The substrate used was n-type silicon with a resistivity of 0.005 Ω cm. 405 nm continuous wave laser diode was used as a light source for LIL. S1813 positive photoresist was spin coated onto the silicon wafer. The thickness of the film was 350 nm. After performing a prebake at 115 $^{\circ}$ C for 60 s and exposing the samples, the patterns were developed in a FM 319 developer, rinsed in deionized water and blow-dried using air. By varying the exposure time and the number and angle of exposure, we fabricated hexagonal and square patterns having different shapes and dimensions. Here, ZnO deposited by RF sputtering was used as a mask for fabrication of patterns (patent no. FR1452514). Reactive ion etching (RIE) was used for silicon etching using ZnO as a mask. SF_6/O_2 gas mixture was used during the RIE etching process.

2.2 Silicon pattern formation using nano-sphere lithography Polystyrene (PS) beads of size 2 μ m

were deposited on the silicon substrate by using dip-coating technique. These beads self-assemble on the surface of silicon. 100 nm thick chromium metal was then deposited on these PS beads. After the metal deposition process, the beads were removed and RIE etching was conducted in order to etch the silicon. In this manner micro-patterns of silicon are formed.

2.3 Growth of ZnO NWs The ZnO seed layer was prepared by mixing a solution containing zinc acetate and ethanol to form a 0.48M solution which was stirred. The seed layer was then deposited on the patterns first by drop coating method and then by spin coating technique. Thereafter, the patterns were annealed on a hot plate at 400 $^{\circ}$ C. The growth of ZnO NWs was conducted by chemical bath deposition technique. 0.025M zinc acetate was dissolved in 250 ml of water and 0.3 ml of ammonium hydroxide was added to the solution and stirred. This mixed solution was heated at 87 $^{\circ}$ C before immersing the sample in this solution for a time period of 15 min. Thereafter, the sample was washed with water and dried in air.

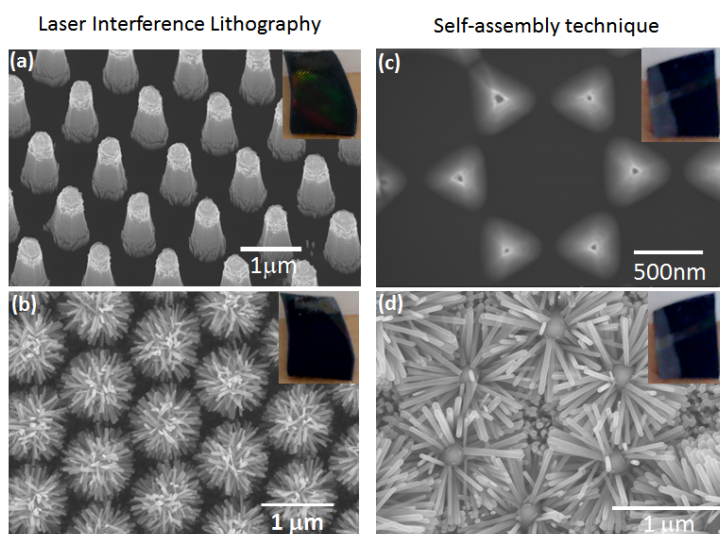


Figure 1 SEM images on the left-hand side show meso-patterns of silicon fabricated by laser interference lithography and after RIE etching. (a) SEM images before and (b) after growth of ZnO NWs. On the right-hand side, SEM images of silicon meso-patterns fabricated by NSL, after metal deposition and etching. (c) SEM image before and (d) after growth of ZnO NWs on these patterns. The insets are the photographs of the corresponding samples.

3 Results and discussion

3.1 SEM imaging Figure 1(a) shows the well-ordered patterns of silicon obtained by LIL technique. The patterns consist on a hexagonal ($P3m1$) distribution of truncated cones with a diameter of 600 nm at the base and 400 nm at the top and a height of 2 μ m. The periodicity is 1 μ m. The inset in the figure shows a photograph of the patterned sample. The bright colours seen in the sample

arise due to diffraction of light from the patterns. Figure 1(b) shows a top view SEM image showing the patterned silicon after the growth of the ZnO NWs with an average diameter of \sim 50 nm and length of \sim 300 nm. The sample appears black in colour after the growth of the NWs as seen from the photograph in the inset of Fig. 1(b). This proves that NWs grown on a patterned silicon surface allow for more light to be absorbed as compared to NWs

grown on an unpatterned silicon surface. NWs grown on an unpatterned silicon surface, show various colours due to thin film interference effects. Results corresponding to the light absorption measurements will be presented in our next manuscript.

On the other hand, Fig. 1(c) shows the ordered patterns of silicon obtained by NSL technique. The patterns consist of a hexagonal array of tetrahedrons with a tetrahedron at each vertex. The tetrahedrons have circumradius of 700 nm and a height of 1.3 μm . The periodicity of these structures is 2 μm . The inset in this figure shows a photograph of the patterned sample. As compared to the inset in Fig. 1(a), these samples do not present any diffraction patterns, which is normal as they are smaller in size and thus less efficient to diffract light. Figure 1(d) shows a top view SEM image showing the patterned silicon after the growth of ZnO NWs. In this case, the ZnO NWs have a diameter of 60 to 80 nm and a length of 450 nm to 600 nm. After the growth of the ZnO NWs the sample looks completely black in colour [Fig. 1(d), inset]. This again proves the enhancement in the absorption of light thanks to the ZnO NWs grown on patterned surfaces.

3.2 X-ray diffraction studies To confirm the phase composition and the crystallinity of the synthesized NWs, we have conducted XRD pattern analysis. Figure 2(a) and 2(b) shows the XRD spectra of the samples obtained by LIL and NSL, respectively (i.e.) Fig. 1(b) and 1(d). The peaks in the XRD spectra in Fig. 2(a) and 2(b) can be assigned to the (100), (002), (101), (102), (110), (103), (112), and (004) crystal planes of ZnO wurtzite crystal structures. The diffraction pattern indicates pure and good crystallinity of the ZnO NWs with the absence of other compounds. The NWs are oriented along the c-axis and are highly crystalline even though the sample is not annealed. For both samples, a powder diffraction-like spectrum is observed which can be easily understood as the NWs orientation is isotropic in the sample plane. Major difference lies in the intensity of the (002) peak which is higher for the NWs grown on the NSL patterned sample [i.e. Fig. 2(b)] as to compare with the intensity of (002) peak of the LIL patterned sample [i.e. Fig. 2(a)]. Following simple geometrical derivation, higher (002) peak intensity could simply be explained by a larger amount of NWs oriented perpendicular to the sample surface in the case of the NSL patterned sample as to compare with the LIL patterned sample [16].

3.3 Photoluminescence studies Room temperature PL spectroscopy was conducted on the two types of samples. He-Cd laser with an excitation wavelength of 325 nm was used for the PL studies. Figures 3(a) and 3(b), respectively, show the PL spectra of the ZnO NWs grown on unpatterned and LIL and NSL patterned silicon. Curves have been shifted for a better reading (cf. the legend). In both cases, a narrow emission peak in the UV at ~ 378 nm and a broad emission peak in the visible with a maximum at

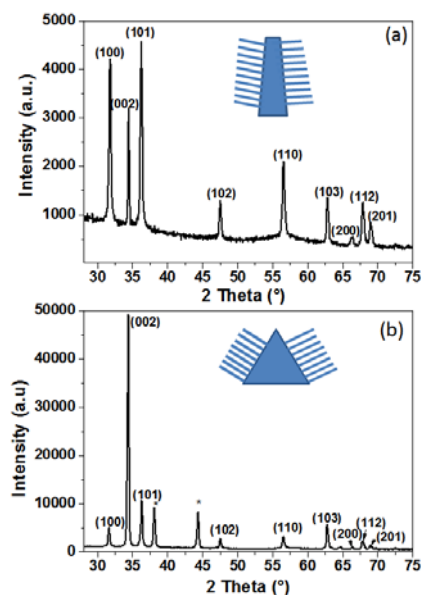


Figure 2 XRD spectra of ZnO NWs grown on (a) Si patterns fabricated by LIL and (b) Si patterns made by NSL technique. The inset in each figure shows schematic of the type of sample studied. The peak marked with asterisk corresponds to diffraction from the sample holder.

~ 610 nm are observed and this whatever the area. These two peaks can be respectively attributed to ZnO near-band edge (NBE) and defect emission. However, defect emission remains lower confirming the good quality of the CBD grown ZnO. It is also worth noting that the unpatterned area give rise to the same signal. The two samples were grown in similar conditions. Indeed a similar crystalline and thus optical quality is expected for the ZnO NWs in both samples. More interestingly, for both cases, we see a clear difference between the unpatterned and patterned area in terms of intensity. While for the NSL pattern sample the integrated signal is higher by a factor of 1.5 for the patterned area as to compare with the unpatterned area, for the LIL patterned sample it is lower by a factor of 0.55. Considering that the amount of luminescence is almost the same for both samples [16], the difference can only be explained by the so-called photonic effect. Before going into details it is important here to note that the PL intensity has been recorded normal to the surface with a collection angle of 16° and therefore mainly sensitive to the radiation pattern normal to the surface. Such a study was recently conducted. Qualitatively such a difference can be explained by the morphology of the silicon patterned substrates and most probably an in-plane reabsorption process. Such enhanced optical absorption is most likely the result of the shape and the high aspect ratio in the LIL patterned sample, as compared to the NSL patterned sample. Nevertheless, further optical studies are to be conducted in order to confirm these assumptions. Quantitative analysis requires an integrated and angular dependent analysis. As a primary

result, optical absorption measurements (not shown here) conducted on these types of heterostructured samples have shown increased light absorption properties. Such structures could facilitate the exploration of novel applications such as improved anti-reflection coatings, owing to both enhanced surface area and better absorption.

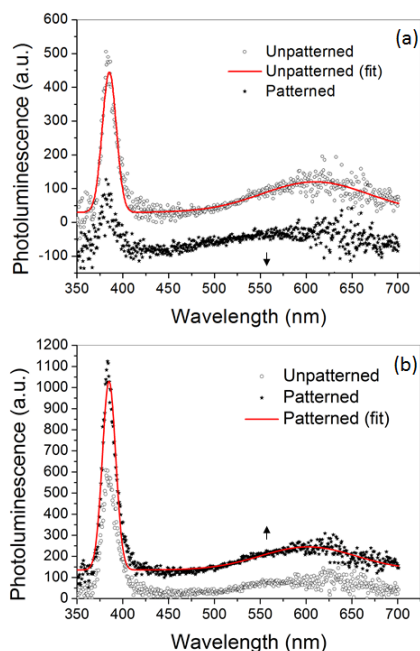


Figure 3 Room temperature PL spectra of ZnO NWs grown on unpatterned and patterned samples using (a) LIL and (b) NSL techniques. As evidenced by the red solid-line curves the spectrum can be explained by two main contributions corresponding to the UV near band-edge emission and visible defect related emission. As indicated by arrows, the spectra have been shifted in intensity for clarity.

4 Summary In this work, fabrication of patterned ZnO NWs has been easily and successfully conducted on mesoscale periodically patterned Si substrates. Substrates were patterned by two different methods, namely laser interference lithography and nanosphere lithography. Ordered patterns of silicon fabricated by LIL show formation of cone-shaped structures of height 2 μm while silicon patterns formed by NSL are tetrahedrons of height 1.3 μm and a base of 700 nm. ZnO NWs having diameters of around 60 nm to 80 nm were grown on these patterns. XRD patterns showed that the NWs are highly crystalline with a wurtzite hexagonal structure and a growth direction along the c-axis. PL spectra show a dominant NBE emission for ZnO NWs grown on both kinds of patterned samples. Lower PL signal recorded on the LIL patterned sample strongly suggests a photonic effect. The emission is reduced in the case of the LIL samples most probably due to an enhancement in the in-plane absorption. In summary, we were able to perform uniform, patterned growth of ZnO

NWs on silicon patterned substrates using bottom-up approach. Such samples appear very interesting for enhancing light-matter interaction. More results on this aspect will be presented in our next article.

Acknowledgements Research reported here was partially supported by the Champagne-Ardennes Region and the European Regional Development Fund through the TEZO (E201211445, E201211419, D201308183 and E201311131) and SYNAPS (D201207251) projects. H. K. would like to acknowledge the ANRT (National Agency for Technical Research) for Ph.D support. All the authors would like to acknowledge the Nano'mat platform for providing the SEM equipment. Mr. Henry Pilliere and Mr. Eric Berthier, (INEL Enterprise, Artenay, France) are also deeply acknowledged for the XRD measurements.

References

- [1] Z. L. Wang, G. Zhu, Y. Yang, S. Wang, and C. Pan, *Mater. Today* **15**, 532 (2012).
- [2] Z. L. Wang, *Adv. Mater.* **24**, 4632 (2012).
- [3] S. Chu, G. Wang, W. Zhou, J. Zhao, J. Kong, L. Li, J. Ren, and J. Liu, *Nature Nanotechnol.* **6**, 506 (2011).
- [4] X. Zhang, M. Lu, Y. Zhang, L. Chen, and Z. Wang, *Adv. Mater.* **21**, 2767 (2009).
- [5] W. Wang, Q. Zhao, H. Li, H. Wu, D. Zou, and D. Yu, *Adv. Funct. Mater.* **22**, 2775 (2012).
- [6] R. Aad, V. Simic, L. Le Cunff, L. Rocha, C. Sartet, V. Sallet, A. Lusson, C. Couteau, and G. Lerondel, *Nanoscale* **5**, 9176 (2013).
- [7] A. Gokarna, R. Parize, H. Kadiri, K. Nomenyo, G. Patriarche, P. Miska, and G. Lerondel, *RSC Adv.* **4**, 47234 (2014).
- [8] Y. J. Hong, S. J. An, H. S. Jung, C. H. Lee, and G. C. Yi, *Adv. Mater.* **19**, 4416 (2007).
- [9] C. Cheng, M. Lei, L. Feng, K. Fung, M. M. Loy, D. Yu, and N. Wang, *ACS Nano* **3**, 53 (2009).
- [10] D. Liu, Y. Xiang, X. Wu, L. Song, W. Y. Zhou, G. Wang, C. Y. Wang, and S. Xie, *Nano Lett.* **6**, 2375 (2006).
- [11] J. Hsu, Z. Tian, N. Simmons, C. Matzke, J. Voigt, and J. Liu, *Nano Lett.* **5**, 83 (2005).
- [12] J. Hwang, S. Cho, E. Seo, J. Myoung, and M. Sung, *ACS Appl. Mater. Interf.* **1**, 2843 (2009).
- [13] D. Yuan, R. Guo, Y. Wei, W. Wu, Y. Ding, Z. Wang, and S. Das, *Adv. Funct. Mater.* **20**, 3484 (2010).
- [14] K. Kim, H. Jeong, M. Jeong, and G.Y. Jung, *Adv. Funct. Mater.* **20**, 3055 (2010).
- [15] H. Kadiri, S. Kostcheev, D. Turover, R. Salas-Montiel, K. Nomenyo, A. Gokarna, and G. Lerondel, *Beilstein J. Nanotechnol.* **5**, 1203 (2014).
- [16] As per our calculations, the quantity of ZnO present (in volume) per unit area is the same in both the samples. For LIL and NSL sample we have a ZnO volume per area unit of 1.07 and 1.06 μm^3 , respectively. The major difference lies in the number of NWs with the c-axis perpendicular to the surface which in volume per area unit is, respectively, 0.23 μm^3 for LIL and 0.52 μm^3 for NSL.